Korean J. Crystallography
Vol. 12, No. 4, pp.227~232, 2001

The Symmetry of Aurivillius Ceramics

Luis Fuentes, Maria E. Fuentes and Hector Camacho
Centro de Investigación en Materiales Avanzados, Chih., México

Abstract

Structure - physical properties relationships for Aurivillius ceramics are discussed, with emphasis in symmetry considerations. Single-crystal materials and polycrystal ceramics are analysed. Electric and magnetic coupling properties are considered. Colour Symmetry Groups and Texture Analysis tools are employed. Symmetry conditions for polarisation vectors and inverse pole figures related to Aurivillius phases are given. The influence of crystallographic texture on the physical properties of polycrystalline Aurivillius ceramics is evaluated.

1. Introduction

Symmetry plays a decisive role in the structure - physical properties relationship of ferroelectric materials. In the case of Aurivillius ceramics, the application of symmetry considerations to structural and technical characterisation is not yet fully systematised. The present paper tends to contribute some useful elements in the indicated direction. Firstly, the proper connection between crystal symmetry and electric polarisation is remarked. Secondly, colour symmetry treatment of magnetic coupling properties is suggested. Finally, the application of symmetry and texture analysis tools to the description of Aurivillius polycrystal samples is illustrated.

2. Single Crystals

Crystal Symmetry and Electric Polarisation. Table 1 resumes the crystallographic characteristics of some representative Aurivillius phases. A wide diversity of crystal-symmetry groups is evident. The last column presents the conditions that are obligatory for the electric dipole moment, in correspondence with the point group that is associated with the reported space group.

The theoretical basis for the electric dipole column of Table 1 resides in the *Neumann Principle* (NP)[11]:

The symmetry group of any macroscopic physical property contains the structure *point group* as a subgroup.

Table 1. Crystallographic data of representative Aurivillius phases and related materials

N	Formula and references	Crystal system	Space group	Point group	Spontaneous polarisation
1	Bi_2WO_6 [1]	O	$P2_1ab$	2mm	P ∥ a
	$Sb_2(W,V)O_{6-x}$ [2]	M	$P2_1/a$	2/m	P = 0
2	$ABi_2Nb_2O_9$ (A = Sr, Ca) [3]	O	$A2_1am$	2mm	P ∥ a
	$BaBi_2Nb_2O_9$ [3]	T	I4/mmm	4/mmm	P = 0
	Bi_3TiNbO_9 [4]	O	$A2_1am$	2mm	P ∥ a
	$Bi_2W_2O_9$ [5]	O	$P2_1an$	2mm	P ∥ a
3	$Bi_4Ti_3O_{12}$ [4]	M	B1a1	m	P ⊥ b
	α-$Bi_4V_2O_{11}$ [6]	M	C2/m	2/m	P = 0
4	$Bi_5Ti_3FeO_{15}$ [7]/[8]	O	F2mm/$A2_1am$	2mm	P ∥ a
5	$Ba_2Bi_4Ti_5O_{18}$ [9]	O	B2ab	2mm	P ∥ a
6	$Bi_7Ti_4NbO_{21}$ [10]	O	I2cm	2mm	P ∥ a

M: Monoclinic; O: Orthorhombic; T: Tetragonal.

For polar vectors and tensors, the mathematical expression of the NP is as follows:

$$A_{ij\ldots m} = \sum_{kl\ldots n} G_{ik}G_{jl}\ldots G_{mn}A_{kl\ldots n} \quad (1)$$

$A_{ij\ldots m}$ is the tensor property under consideration and G_{ik} represent the rotation matrices of the structure point group.

The NP leads to important consequences in relation to the physical properties of Aurivillius phases.

A well-known fact is that for crystals belonging to centric point groups the occurrence of spontaneous polarisation is impossible. These crystals are not allowed to exhibit pyro- ferro- or piezoelectricity.

The following rule also follows from the NP. Unfortunately, adherence to it is not systematically observed in published reports.

For crystals belonging to any space group associated with point group 2 mm, the spontaneous polarisation vector ***P*** points necessarily parallel to the two-fold rotation axis ("***a***"). Components of ***P*** non-parallel to ***a*** are impossible in this type of crystals.

The application of the mentioned conditions to the analysis of Aurivillius phases crystal structures would lead to the improvement of a number of determinations, for example, of those reported in.[3,6,9]

Magnetic Coupling Effects and Colour-symmetry Point Groups. The possible occurrence of pyromagnetic ($dB_j = i_j\, d\theta$), magnetoelectric ($B_i = m_{ij} E_j$) and piezomagnetic ($B_i = b_{ijk}T_{jk}$) effects in Fe-containing Aurivillius crystals motivates at present basic and technological interest. Just written symbols have the following meaning: B_j: magnetic induction vector; i_j: pyromagnetic coupling vector; q: temperature; b_{ijk}: piezomagnetic tensor; T_{jk}: mechanical stress; m_{ij}: magnetoelectric tensor; E_j: electric field intensity.

Concentric tetrahedra in Fig. 1 schematically represent elastic, thermal, electric and magnetic coupling properties. Conventional "effect" magnitudes lie in the inner spheres, while "cause" quantities are on outer ones. "Cause-effect" coupling relations are represented by discontinuous lines. Continuous black lines denote "cause-cause" and "effect-effect" links. Broad gray lines are associated to so-called "principal" actions, relating quantities of the same nature.

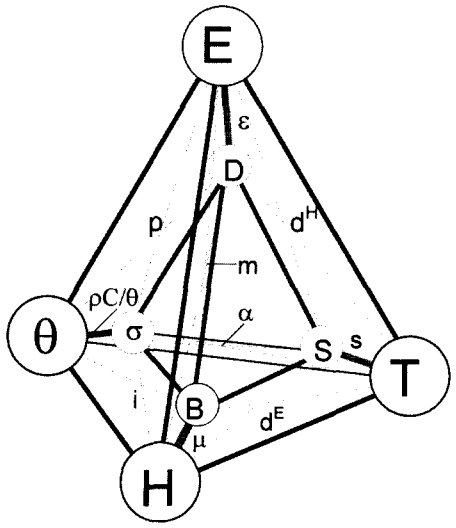

Fig. 1. Schematic representation of constitutive relations for equilibrium properties.

Magnetoelectric effect is gaining attention due to its potential applications, as well as for the basic questions it poses. The low-frequency manifestation of this phenomenon may be characterised by means of an elastic connection between piezoelectric and piezomagnetic effects. In simplified notation and with the help of Fig. 1, the following relations express this idea symbolically.

$$\begin{aligned} &B = mE \qquad m = eb \;\; (T = eE) \\ &e = dc \;\; (c = s^{-1}) \\ &m = ds^{-1}b \end{aligned} \quad (2)$$

Experimental investigations on the magnetic coupling properties of Aurivillius ceramics are in their initial stages.[12-14] The following is a brief mention of symmetry considerations to be taken into account in the study of the mentioned physical effects.

The magnetic coupling factors i_j, m_{ij} and b_{ijk} are, respectively, first-, second- and third-rank ***axial*** tensors. The behaviour of axial vectors and tensors under symmetry operations shows interesting differentiating characteristics. An axial vector does not invert itself under the inversion operation. While a polar vector is always parallel to a normal symmetry plane, an axial vector is normal to such a plane.

Symmetry investigations of magnetic phenomena

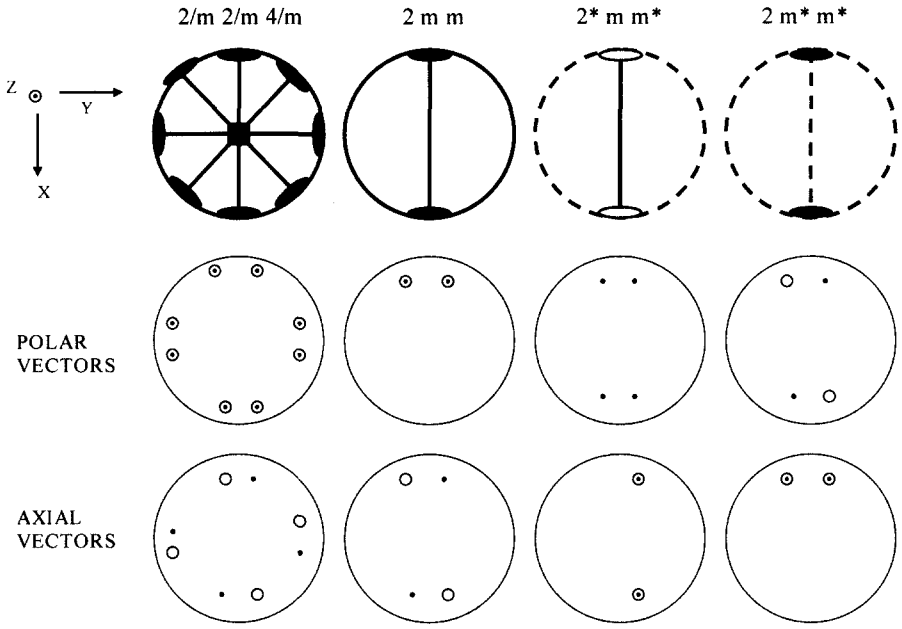

Fig. 2. Polar- and axial-vectors symmetry. Selected tetragonal and orthorhombic colour point groups.

must include colour-symmetry categories and rules.

Figure 2 represents, by means of stereographic projections, diagrams that show the symmetry behaviour of polar and axial vectors for the colour-symmetry groups that are possible in Aurivillius 2 mm crystals. The first row describes the colour symmetry elements, as follows. Filled square: fourth-order symmetry axis; filled boat; second-order symmetry axis; void boat: anti-symmetry second-order axis; continuous gross line or circumference: mirror; discontinuous line: anti-mirror. The second and third rows present the directions that are generated by the considered colour-symmetry operations. Points show orientations towards the North hemisphere while empty circles denote South oriented ones.

The axial nature of magnetic properties leads to the following modification of the analytical conditions to be fulfilled by the considered magnitudes.

$$B_{ij\ldots m} = |G| \sum_{kl\ldots n} G_{ik}G_{jl}\ldots G_{mn}B_{kl\ldots n} \qquad (3)$$

$B_{ij\ldots m}$ is the axial tensor property.

The tensors of all physical properties satisfy equations (1) or (3) (depending on the polar or axial nature of the considered property) with G_{jk} scanning all the colour-symmetry operations of the structural colour point group.

Table 2 may be obtained with the help of conditions (1) and (3). It resumes the possible electric and magnetic coupling effects in the 32 crystallographic point groups. Rows corresponding to Aurivillius phases are shaded. In electric as well as in magnetic cases, pyro-susceptible materials are a sub-set of piezo- susceptible ones.

3. Polycrystal Ceramics

Texture and Polarisation Description. Analytical tools of Texture Analysis are suggested as appropriate instruments for characterisation of structure and physical properties in ferroelectric polycrystals.[15,16] The central magnitude for the description of texture is the *orientation distribution function* (ODF) *f(g)*. This quantity represents the volume fraction of crystallites (or domains) in the neighbourhood of a given orientation *g*:

$$f(g)\ dg = dV/V \qquad (4)$$

Polycrystal symmetry is a combined result of crystal symmetry and texture symmetry. The ODF

Tabl 2. Electric and magnetic coupling effects crystallographic point groups

	Point group							
Cryst. Syst.	Int	Sch	type	PRE	PZE	PRM	PZM	ME
triclinic	1	C_1	e	+	+	+	+	+
	$\bar{1}$	C_i	c			+	+	
monoclinic	2	C_2	e	+	+	+	+	+
orthorhombic	222	D_2	e		+		+	+
	mmm	D_{2h}	c				+	
tetragonal	4	C_4	e	+	+	+	+	+
	$\bar{4}$	S_4	nc-ne		+	+	+	+
	4/m	C_{4h}	c			+	+	
	422	D_4	e		+		+	+
	4mm	C_{4v}	nc-ne	+	+		+	+
	$\bar{4}$2m	D_{2d}	nc-ne		+		+	+
trigonal	3	C_3	e	+	+	+	+	+
	$\bar{3}$	S_6	c			+	+	
	32	D_3	e		+		+	+
	3m	C_{3v}	nc-ne	+	+		+	+
	$\bar{3}$m	D_{3d}	c				+	
hexagonal	6	C_6	e	+	+	+	+	+
	$\bar{6}$	C_{3h}	nc-ne		+	+	+	
	6/m	C_{6h}	c			+	+	
	622	D_6	e		+		+	+
	6mm	C_{6v}	nc-ne	+	+		+	+
	$\bar{6}$m2	D_{3h}	nc-ne		+		+	
	6/mmm	D_{6h}	c				+	
cúbic	23	T	e		+		+	+
	m3	T_h	c				+	
	432	O	e					+
	$\bar{4}$3m	T_d	nc-ne		+			
	m3m	O_h	c					

Legend : Int : international notation; Sch : Schoenflies notation; e : enantiomorphic; c : centric; nc-ne : non centric-non enantiomorphic. + : possible; PRE : pyroelectricity; PZE : piezoelectricity; PRM : pyromagnetism; PZM : piezomagnetism; ME : magnetoelectric effect.

is invariant under *proper rotations* (inversion not included) that belong to the considered *ordinary-symmetry* point groups. Let the proper rotations from crystal symmetry be denoted by G^c and those from texture symmetry by G^t. Then the following relation holds:

$$f(g) = f(G^t \bullet g \bullet G^c) \tag{5}$$

Fibre textures are completely characterised by means of the fibre axis *inverse pole figure* (IPF) ***R(h)***. ODFs and IPFs are measured by neutron, x-ray or electron diffraction. *Ghost-texture* corrections are generally required.[15]

Figure 3 represents, by means of inverse pole figures, the symmetry changes that take place in a hypothetical textured Aurivillius ceramic during a poling procedure. The considered model sample has been obtained by hot forging. It shows fibre (0, 0, 1) texture. Sample direction for all IPFs is parallel to the direction of pressure application. Polarising field is also applied in this direction.

The starting condition is at a temperature above

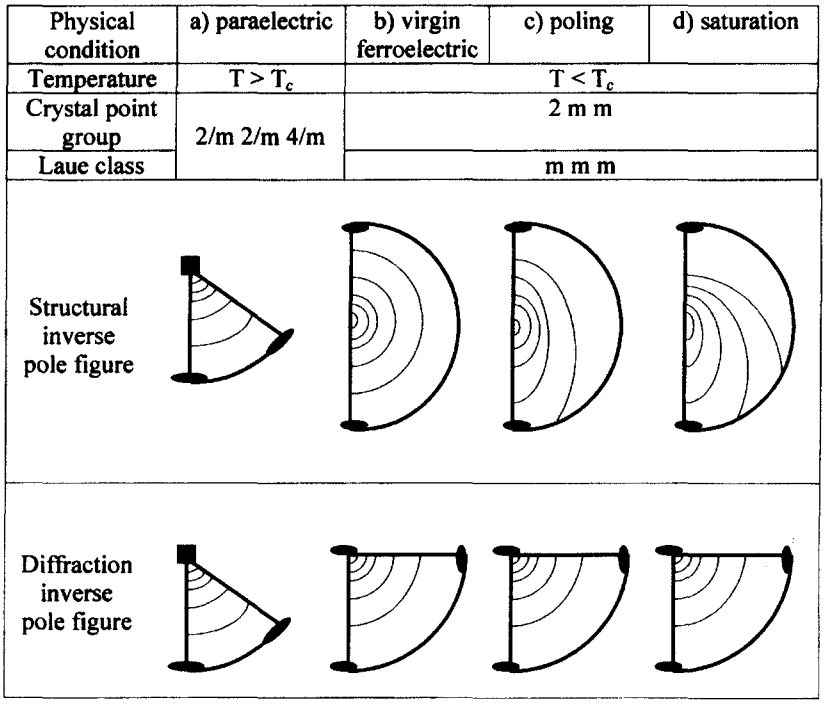

Fig. 3. Texture description of polarisation process. Hot forged Aurivillius ceramic.

the Curie point, $T > T_c$. The inverse pole figure irreducible region that is shown corresponds to point group 2/*m*2/*m*4/*m*. The constant-density lines indicate higher population densities in the vicinity of crystal direction (0, 0, 1).

By cooling the sample, $T < T_c$, the structural IPF irreversible region enlarges itself as corresponds to 2*mm* point group. Due to Friedels law, the diffraction IPF shows *mmm* (2/*m*2/*m*2/*m*) symmetry. In the virgin ferroelectric condition, the statistical symmetry of all the IPF coincides with that of the paraelectric structure (4/*mmm*).

On poling, the structural IPF experiences a breakdown of the statistical *mmm* symmetry. Favourably oriented domains grow by expanding their borders into non-favourably oriented regions. Diffraction is not sensitive to this phenomenon, so diffraction IPF remains invariant during poling.

Macroscopic Physical Properties. Polycrystal physical properties are averaged from single-crystal ones.[17-20] The weight function is the ODF *f(g)*. The following formulae resume a polycrystal property calculation for a highly-symmetrical case. The considered situation is a fibre texture problem, under the ordinary average surface description (15). The macroscopic (average) property associated to a given sample direction *y*, $\overline{E}(y)$, is given by a spherical harmonics expansion:

$$E(y) = \sum_{l=0}^{r} \sum_{\nu} \xi_l^{\nu} k_l^{\nu}(y) \tag{6}$$

ξ_l^{ν} are property expansion coefficients and represent symmetry-adapted spherical harmonics.[21,22] The tensor associated to property E is of rank r. Property coefficients are given by:

$$\xi_l^{\nu} = \frac{1}{2l+1} \sum_{\mu} C_l^{\mu\nu} e_l^{\mu} \tag{7}$$

C_l^{μ} and e_l^{μ} are, respectively, IPF and single crystal property expansion coefficients. Equation (7) expresses the mathematical dependence of polycrystal properties on single crystal characteristics and texture.

Figure 4 represents an application of Texture Analysis methods to the characterisation of texture-

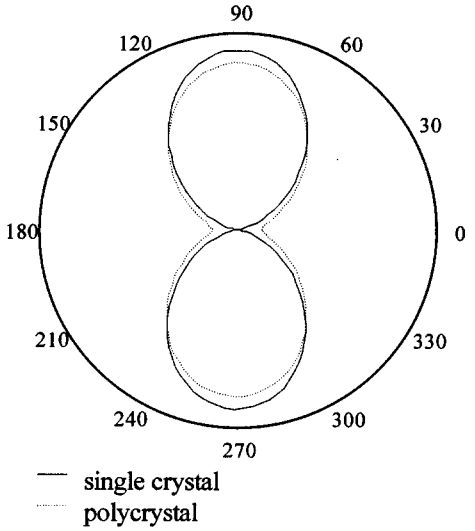

Fig. 4. Dielectric constant surface representations. Single crystal and textured polycrystal ceramic of $PbBi_4Ti_4O_{15}$. The symmetry group of both surfaces is ∞/mmm, in accordance with the Neumann Principle.

modulated properties for an Aurivillius polycrystal. Selected study case has been taken from.[23] Single crystal and polycrystal ceramic dielectric constants are represented by means of the longitudinal dielectric modulus $\varepsilon(h)$. Continuous curve corresponds to 1 MHz single crystal parameters, as given by the mentioned reference ($\varepsilon_{11} = \varepsilon_{22} = 18300$; $\varepsilon_{33} = 430$). Dashed curve describes the dielectric modulus of a modelled Gaussian (0, 0, 1) fibre texture. Average values of $\varepsilon(h)$ were calculated with the help of equations (6) and (7). The width Ω of the crystallite orientation distribution has been fitted to $\Omega = 23°$. This value is such that, for the polycrystal, $\varepsilon_{33} = 3000$, as in.[23]

Acknowledgements

Present investigation has been supported by the Consejo Nacional de Ciencia y Tecnología de México, CONACYT - Project 31234-U and by CYTED - Red Iberoamericana de Electrocerámicas. Support is gratefully acknowledged.

References

1) Knight, K. S., *Ferroelectrics*, **150**, 319 (1993).
2) Ramirez, A., Enjalbert, R., Rojo, J. M. and Castro, A., *J. Solid State Chem.*, **128**, 30 (1997).
3) Blake, S. M., Falconer, M. J., Mccreedy, M. and Lightfoot, P., *J. Mater. Chem.*, **7**, 1609 (1997).
4) Withers, R. L., Thompson, J. G. and Rae, A. D., *J. Solid State Chemistry*, **94**, 404 (1991).
5) Champarnaud-Mesjard, J.-C., Frit, B. and Watanabe, A., *J. Mater. Chem.*, **9**, 1319 (1999).
6) Joubert, O., Jouanneaux, A. and Ganne, M., *Mater. Res. Bull.*, **29**, 175 (1994).
7) Kubel, F. and Schmid, H., *Ferroelectrics*, **129**, 101 (1992).
8) Ko, T., Ch. Jun and Lee, J., *Korean J. Ceram.*, **5**, 341 (1999).
9) Irie, H., Miyayama, M. and Kudo, T., *J. Am. Ceram. Soc.*, **83**, 2699 (2000).
10) Mercurio, D., Trolliard, G., Hansen, T. and Mercurio, J. P., *Int. J. Inorg. Mater.*, **2**, 397 (2000).
11) Nowick, A. S., *Crystal Properties Via Group Theory*, Cambridge Univ. Press, Cambridge (1995).
12) James, A. R., Kumar, G. S., Kumar, Mahendra, Suryanarayana, S. V. and Bhimasankaram, T., *Modern Physics Letter*, **B 11**, 633 (1997).
13) Srinivas, A., Suryanarayana, S. V. and Kumar, Mahesh, *J. Phys.: Condens. Matter*, **11**, 3335 (1999).
14) Kumar, Mahesh, Srinivas, A. and Suryanarayana, S. V., *J. Phys.: Condens. Matter*, **11**, 8131 (1999).
15) Bunge, H. J., *Texture Analysis in Material Science*, Butterworths, London (1982).
16) Fuentes, L. and Raymond, O., *Textures and Microstruct.*, **23**, 221 (1995).
17) Bunge, H. J., *Materials Science Forum*, **273-275**, 3 (1998).
18) Diz, J. and Humbert, M., *J. Appl. Cryst.*, **25**, 756 (1992).
19) Humbert, M., Wagner, F., Philippe, M. J. and Esling, C., *Text. and Microstruct*, **14-18**, 443 (1991).
20) Van Houtte, P., *Materials Science Forum*, **273-275**, 67 (1998).
21) Raymond, O., Fuentes, L. and Gómez, J. I., *Textures and Microstruct.*, **28**, 81 (1996).
22) Raymond, O., Fuentes, L. and Gómez, J. I., *Textures and Microstruct.*, **28**, 93 (1996).
23) Yi, I.-S. and Miyayama, Masaru, *Materials Res. Bull.*, **32**, 1349 (1997).